BOR DERGİSİ

JOURNAL OF BORON

The synthesis of NiO@N-doped reduced graphene oxide and its application for hydrogen generation from ammonia borane

Derya Öncel Özgür[1*]

[1]Gazi University, Department of Chemical Engineering, Ankara, 06570 Turkey,
ORCID orcid.org/0000-0001-5490-0707

ARTICLE INFO

ABSTRACT

Ammonia borane (AB) is considered a highly promising candidate among the chemical hydrogen storage compounds. The improvement of efficient and low-cost catalysts is key to comprehending a highly efficient hydrogen generation reaction. In this study, the synthesis of non-noble nickel oxide on nitrogen-doped graphene (NiO@N-rGO) was carried out and its efficiency towards the catalytic dehydrogenation of AB was investigated under mild conditions (25-50°C). The synergic effect between NiO and nitrogen-doped rGO has increased the performance of the catalyst. As a result, the turnover frequency (63 mol H_2 min^{-1} (mol Ni)$^{-1}$ of NiO@N-rGO) is which higher than most of the Ni-based catalyst. The activation energy (E_a) measured to be 48.7 kJ mol^{-1} is among the values of the most active catalysts.

1. Introduction

The fuel cell has been widely recognized as highly favorable for large energy systems for many years, however, the recent concern has focused on the small portable power sources [1]. It was postulated that the hydrogen-based portable or mobile energy systems would be desirable to utilize by using chemical hydrides. Up to now the most of the chemical hydride surveys have been conducted taking into consideration the hydrolysis of $NaBH_4$ due to several advantages [2-6]. Although $NaBH_4$ appears an attractive candidate for portable or mobile devices under mild conditions, it suffers from the requirement of a highly basic NaOH solution which ensures its chemical stability to avoid self-hydrolysis in water [7].

Scientific approaches demonstrated that the most applicable method to overcome the main challenges on the on-board system has been viewed as chemical hydrogen storage [8]. Among them, B-N-H compounds, especially the ammonia-borane complex, (AB, NH_3BH_3) has received increasing attention as a promising for on-board hydrogen application due to having high hydrogen content (19.6 wt%), eco-friendly source, and high stability as opposed to $NaBH_4$ [9]. After the synthesis of AB in 1955 [10], it has been used as the reducing agent [11] and the main precursor to produce the other boron-containing materials, such as metal amidoborane [12], however, the interest in AB has un-expectedly shifted to its capability as a high-capacity of hydrogen storage materials. The electronegativity discrepancy between nitrogen and boron accounts for the polarization of the hydrogens in AB, the hydridic B-H, and protic N-H, readily leading to dissociation of B-N bonding and consequently promoting the hydrogen releasing [13]. The releasing hydrogen from AB in a general approach could be carried out in two methods: (i) thermolysis at a higher temperature (ii) the catalytic release in the non-aqueous solvent or aqueous solvent named the hydrolysis. The hydrolysis reaction could release up to 3 moles hydrogen per 1 mole of AB only in the presence of an appropriate catalyst at the ambient condition.

There appears to be numerous data published up to this point regarding noble metals, transition metals, and their bimetallic or multimetallic hybrids. Among the catalysts tested, it can be made inferences that noble based metal catalysts such as Pt, Rh, Ru, or Pd exhibit the highest activity than that of most transition-based metal catalysts toward AB hydrolysis. Hence, for practical use, the inexpensive and efficient catalytic materials are a favorable substitute for precious-metal-based catalysts. It was recently found that the rational design of the bifunctional or multifunctional combination including transition metals or other counterparts (oxides, hydroxides, and phosphides) and carbon-based materials makes the transition metals competitive for increasing the catalytic reactivity [14].

*Corresponding author: deryaoncel@gazi.edu.tr

Among the transition metals, Ni-based catalyst has been considered as one of the most promising candidates. However, the success of nano-based catalyst strongly depends on the stability of Ni nanoparticles (NPs) since the nano-size particles tend to build-up more stable agglomerates, which could lead to loss of active sites and show somewhat lower catalytic activity. It is well accepted that those kinds of problems could be modified with the incorporation of supports like carbon [15], graphene oxide [16], carbon nanotubes [17]. So far, only a few studies have investigated the effect of nitrogen-doped graphene oxide as a supports [18,19]. The present study aims to offer that the hybrid structured nitrogen-doped reduced graphene oxide (N-rGO) could be an proceeding support for enhancing the catalytic activity of NiO nanoparticles. This perspective for the first time emphasizes the rational design of NiO@N-doped reduced graphene oxide nanoparticles for the hydrogen generation form AB. Regarding the proposed model, NiO can enable the adoption of H_2O (H-OH) with dissociation proceeding favorably, and N-rGO would render electron interactions as an conductive support, thus reveals the synergic effects. A graphene-based assemble has been considered as ideal supporting material due to its outstanding intrinsic properties such as a large surface area with a tunable nanoscale morphology and porosity and good electrical conductivity [19,20]. Furthermore, the surface of nitrogen-doped rGO with extraordinarily electronic and chemical structure could possess a substantially high positive charge on the carbon atoms adjacent to nitrogen dopant. This helps the further improvement of the catalytic performances of NiO-based catalysts. Given the aforementioned design, it would be expected that the NiO@N-rGO would provide kinetically accelerating the hydrogen evaluation rate from AB.

2. Materials and Methods

2.1. Synthesis of Nitrogen-Doped Reduced Graphene Oxide (N-rGO)

The synthesis of graphene oxide (GO) from flake graphite powder was carried out by using a modified Hummers' method [21,22]. As-synthesized GO (100 mg in 50 mL water) was dispersed by sonication for 30 min. Then, 100 mg of urea was added with magnetically stirring for 12 hours. The mixture was then transferred into a Teflon-sealed autoclave and kept at 180°C for 12 hours. The nitrogen-doped graphene sheets were centrifuged and obtained after being washed with deionized water several times. Finally, the collected samples were dried in the oven at 60°C to obtain in powder form and denoted as N-rGO.

2.2. Synthesis of Nickel Oxide Nanocomposites on Nitrogen-Doped Reduced Graphene Oxide (NiO@N-rGO)

As-synthesized 20 mg N-rGO in the previous stage was put into the 30 mL of water in a flask and kept under ultrasound for 30 min. As the percent of Ni content was to be 20% by weight, the required amount of $NiSO_4.6H_2O$ was then added into the mixed solution and heated up to 60°C, and kept at this temperature during the reduction. The pH was adjusted to 10 with 0.5 M NaOH before initiating the reduction with hydrazine hydrate. The reaction started when the 2 mL of hydrazine hydrate was added to the flask with stirring for 6 hours at 60°C. The sample was centrifuged and wash using distilled water at least three times. The final product was named NiO@N-rGO after drying in an oven at 60°C.

2.3. Structural Characterization

The structure of the as-prepaid composites was characterized by X-ray diffraction (XRD) by employing Cu-Kα radiation with λ at 1.5418 Å; and X-ray photoelectron spectroscopy (XPS) data collected on an X-ray photoelectron instrument (K-alpha, Thermofisher Scientific Company) equipped with Al Kα radiation at a power of 150 W and a voltage of 12 kV. FT-IR analaysis was applied on a dry powder equipped with a KBr beam splitter in the frequency range of 4000 to 650 cm^{-1} at room temperature. The surface structure characterizations were performed on a Quanta 400F Field Emission scanning electron microscope.

2.4. Hydrogen Generation Measurements

The volume of hydrogen releasing during the dehydrogenation of AB in the presence of NiO@N-rGO catalysts was determined by monitoring the traditional water-displacement method. In a typical experiment, NiO@N-rGO catalyst (10 mg in 5 mL water) was introduced into the three-necked round-bottom flask and magnetically stirred. The reaction temperature was kept constant at the desired setting during all reaction periods by using a water bath. Once the solution of AB (0.15 M, 10 mL) was inserted into the reaction medium via the pressure equalization apparatus, the hydrolysis reaction simultaneously took place and recorded the volume of the hydrogen.

3. Results and Discussion

3.1. Characterization of NiO@N-rGO

The X-ray diffraction (XRD) patterns of the NiO@N-rGO, GO, and N-rGO are shown in Figure 1a and Figure 1c. The GO has a sharp diffraction peak centered at 2θ=11.1° in Figure 1c, yet, this peak entirely disappeared and a broad peak located at around 24.5° indexed to the (002) plane of graphitic materials was ascertained for both reduced samples (N-rGO and NiO@N-rGO), confirming the arrangement of the graphitic crystal with composed of few-layer stacked graphene nanosheets [23]. Nitrogen doping in graphene leads to consisting of defect site and destructing of carbon lattice, which turns out to be low crystallinity as shown in Figure 1a [24]. The XRD pattern of NiO major diffraction peaks is ascribed to NiO(111),

NiO(200), NiO(220), and NiO(311), respectively [25]. The mean particle size of NiO nanoparticles was calculated by using the Debye-Scherrer's formula [26] $(D=0.89/(\beta\cos\theta))$ where β is the full width at half maximum (FWHM), taken in radians, λ is 1.5418 for Cu-Kα radiations. The mean particle size obtained from the reflection (200) at 43.5° is 2.6 nm and the most intense reflection (220) is 5.4 nm.

FTIR spectroscopy was performed to investigate the functional groups in the NiO@N-rGO hybrids. As shown in Figure 1b, the spectrum of NiO@N-rGO shows (i) a broad peak at 3425 cm^{-1}, and a peak at 1627 cm^{-1} which is a typical stretching vibration and bending vibrations of hydroxyl groups, respectively [27,28] (ii) Absorption peaks at 2923 and 2850 cm^{-1} due to the C-H stretching mode of the CH$_2$ groups [24] (iii) the peak is at 1265 cm^{-1} belongs to of the C-N bond, indicating that nitrogen atoms were successfully doped into the carbon matrix [29] (iv) the C-N stretching and N-H stretching at 1382 and 1462 cm^{-1} respectively [24] (v) the bands around 624 and 470 cm^{-1} belongs to the Ni-O vibrations and Ni-O-H bending vibrations, individually [30,31]. The FTIR observation indicates both the addition of nitrogen heteroatom in rGO and the evidence of NiO on the surface of N-rGO.

X-ray photoelectron spectroscopy (XPS) was used to search the detailed surface chemical composition and the oxidation state of the NiO@N-rGO hybrid composite (Figure 2). The survey spectrum (Figure 2a) confirms that the as-prepared NiO@N-rGO is comprised of C, N, O, and Ni elements. Corresponding to the survey XPS measurements, the weight percentages of C, N, O, and Ni in the composite are found as 63.11, 1.95, 31.02, and 3.40 wt%, respectively. Figure 2b displays the C 1s spectrum displays the five deconvoluted peaks of C atoms. The main carbon peak at 284.8 eV seems to be predominantly C-C bond with sp^2 hybridization as indicated by the presence of graphene [32]. The other peaks have appeared at 285.8 eV, 286.6 eV, and 287.9 eV coincided with C-N, C=O, C-O (287.9 eV), and O-C=O (289.1 eV) [33] species, respectively. Besides, the N 1s spectrum in Figure 2c exhibits three peaks at 398.1, 399.5, and 400.8 eV, designated to the pyridinic N, pyrrolic N, and graphitic N, which are the typical three sates of N elements incorporated into rGO [32]. The Ni 2p XPS spectra (Figure 2d) presents the characteristic 2$p_{3/2}$ and 2$p_{1/2}$ doublet caused by spin-orbital coupling. Moreover, their satellite at 861.59 eV and 879.78 eV are observed, which proving the existence of NiO [34,35]. As a result, it is sensible to infer that the NiO@N-rGO composite was synthesized.

The scanning electron microscopy (SEM) analysis was utilized to elucidate the surface morphological properties and microstructure of the as-prepaid catalysts. The higher magnification SEM images in Figure 3a clearly demonstrated the existence of the ripped and wrinkled sheets as proof of the nitrogen-doped rGO with exfoliated few layers. Meanwhile, Figure 3b also confirmed that the NiO particle was uniformly anchored onto the graphene sheets.
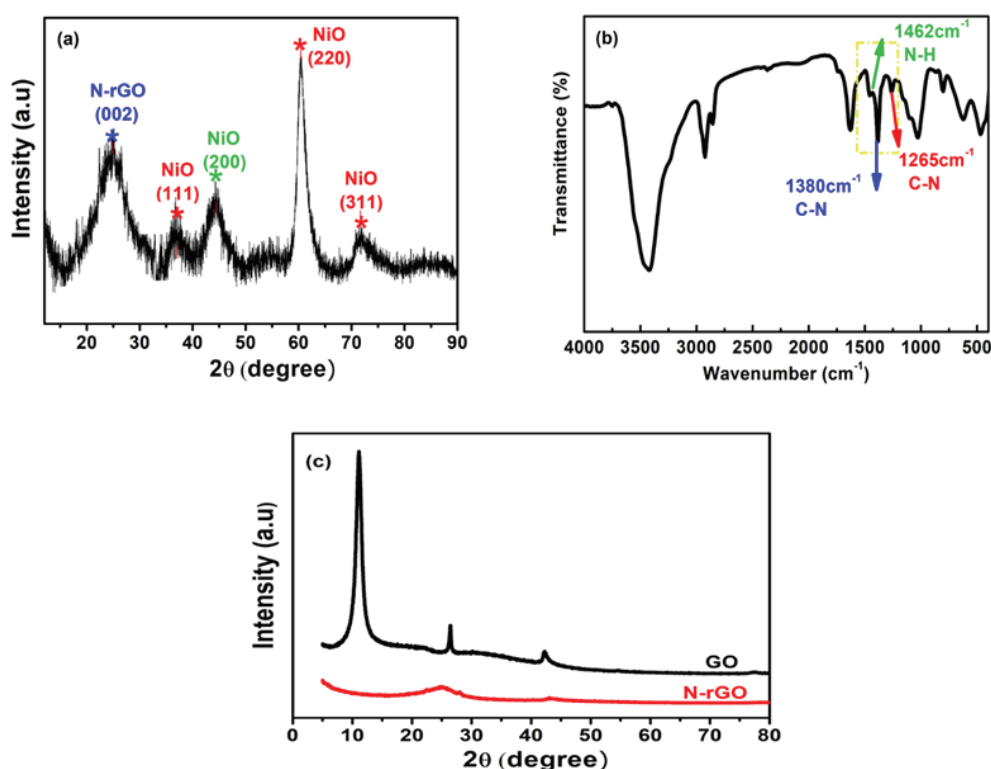
Figure 1. (a) The XRD and (b) FTIR spectra of the NiO@N-rGO (c) XRD spectra of GO and N@rGO.
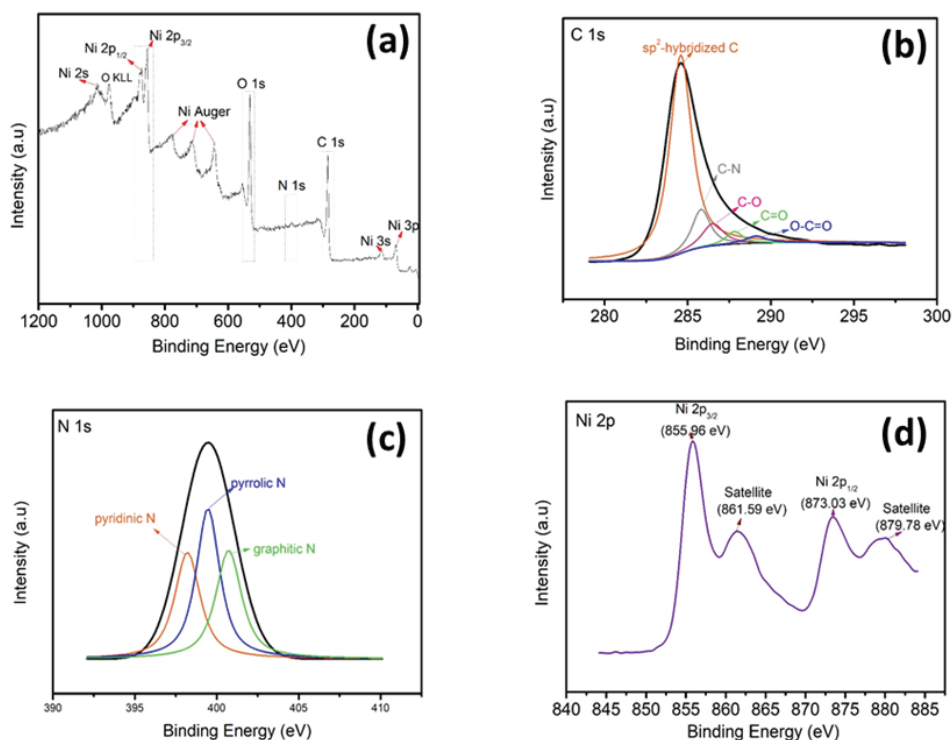
Figure 2. XPS measurements (a) Survey spectra of NiO@N-rGO (b) High resolution C 1s XPS spectra; (c) High resolution N 1s XPS spectra; (d) High resolution Ni 2p XPS spectra.

3.2. Catalytic Activities for Hydrolysis of AB Over NiO@N-rGO

The catalytic activities for hydrolysis of AB were investigated by monitoring the amount of H_2 evaluation at regular intervals. Figure 4a represents the plots of the volume of hydrogen collected gas versus the reaction time in the presence of the as-prepaid NiO@N-rGO catalyst, indicating high catalytic activity for the hydrolysis reaction of AB. Except for the room temperature measurements, it was observed that nearly 3 equivalent of hydrogen per ammonia borane was released in 40 min in Figure 4b, corresponding to the turnover frequency (TOF) value of 63 mol H_2 min^{-1} (mol Ni)$^{-1}$ at temperatures above 25°C. The TOF values and activation energies of the hydrolysis of AB solution catalyzed by previously reported Nickel-based catalysts are summarized in Table 1 for comparison. The TOF value of NiO@N-rGO catalyst is higher than most previously published non-noble Ni metal-based NPs (Table 1) and even many noble metal-based NPs [36-38]. The results confirm that the positive synergistic effect between N-doped rGO and NiO NPs was improved the hydrogen production rate during AB dehydrogenation.

As shown in Figure 5, plotting the initial and final concentration differences versus time result in a straight line under our experimental conditions, implying that the hydrolysis of AB over NiO@N-rGO is a zero-order reaction with regard to AB concentration, and could be described as Eqn. 1. It means that the hydrogen production rate is controlled by the surface reaction. It is well accepted the apparent activation energy is another important factor influencing the reaction kine-
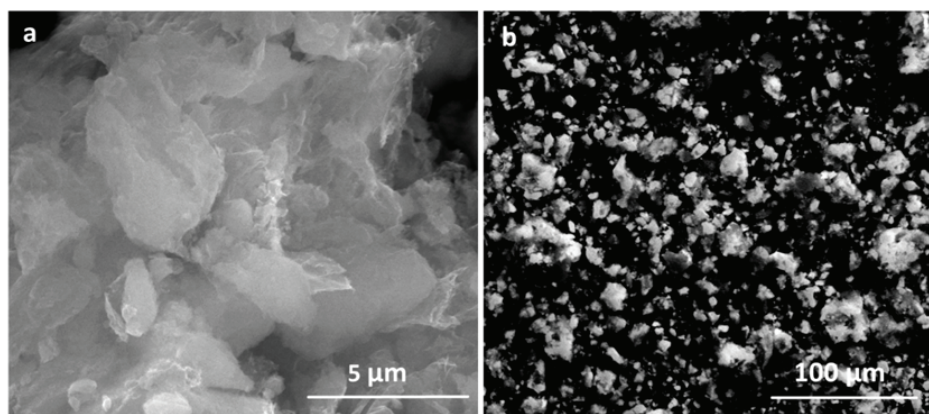
Figure 3. SEM micrographs of the NiO@N-rGO catalyst with a) 5 μm scale b) 100 μm scale.
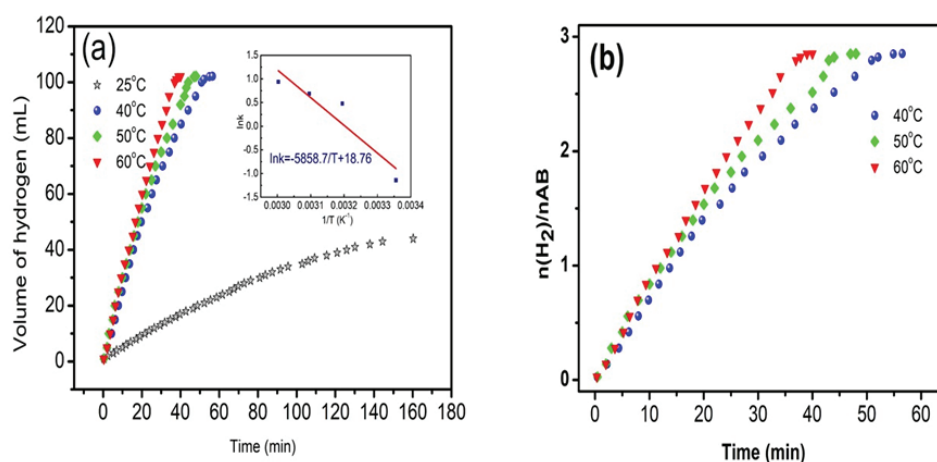
Figure 4. (a) Volume of H$_2$ during hydrolysis of AB as a function of time over NiO@N-rGO at different temperatures and the Arrhenius equation of ln *k versus* 1/T (b) The curves of equivalents H$_2$ per mole of AB over NiO@N-rGO at different temperatures.

tics. Moreover, the reaction rate constant k could be associated with activation energy (E$_a$) by the Arrhenius equation (Eqn. 2). The rate constant k's at various temperatures in the range 25-60°C were determined from the slope of the linear part of each plot (Figure 5). The inset of Figure 4a displays the lnk vs 1/T (Arrhenius plot), from which the activation energy was calculated to be 48.7 kJ·mol^{-1}. The activation energy value of the as-prepaid NiO@N-rGO catalyst is acceptable if compared to that of other Ni-based catalysts in Table 1. A: pre-exponential factor, R: universal gas constant, and T: temperature in K.

$$r = \frac{-3d[NH_3BH_3]}{dt} = \frac{d[H_2]}{dt} = k \qquad (1)$$

$$k = A exp(-\frac{E_a}{RT}) \qquad (2)$$

The improved activity of the as-prepaid catalyst could be originated from three main reasons: (I) the small size of the particles by calculating the Debye-Scherrer equation, leading to a better dispersion on the graphene support (II) NiO could easily promote the adsorption of water (H-OH), in which hydrogen turns out to be electropositive. This initiation steps forward the reaction into the tempt of electronegative H in AB [14], and help the further hydrolysis to attack the B-N bonds [49] (III) The interaction between NiO and N-rGO could build up a new electronic structure, which differs from their pure states [49]. Meanwhile, it was suggested that with the incorporation of any metallic compound such as Ni, or Pt by acting as a bridge between NiO and graphene layer, the reaction kinetics would further accelerate by facilitating the electron transfers.

4. Conclusions

In summary, this study demonstrated a facile method for the synthesis of nitrogen-doped graphene oxide supported NiO nanocomposites, and their activities against hydrogen production from the AB under mild conditions. The nitrogen-doped rGO was synthesized in a one-pot hydrothermal method by using urea as reducing-doping agents. NiO NPs were anchored onto N-rGO by reduction method with hydrazine hydrate. Moreover, this method can be widespread usage of the other graphene supported NPs for future applicati-

Table 1. Activities in terms of TOF and activation energy values of the Ni-based catalysts used for the hydrolysis of AB.

Catalysts	TOF (molH$_2$ molcat^{-1} min^{-1})	E$_a$, (kJ/mol)	Reference
NiO@N-rGO	63	48.7	This study
Ni sphere	19.6	27	[39]
Ni/C	8.8	28	[40]
NiCl$_2$	0.40	-	[41]
PVP stabilized Ni NPs	4.5	-	[42]
NiP/rGO	13.3	34.7	[43]
Ni/SiO$_2$-CoFe$_2$O$_4$	5.3	68.2	[44]
Ni/BN	1.25	63.2	[45]
Ni/Ni$_2$P	68.3	44.99	[46]
Ni@TiN-NTs	11.73	52.05	[47]
Ni$_{12}$P$_5$	23	50.4	[48]
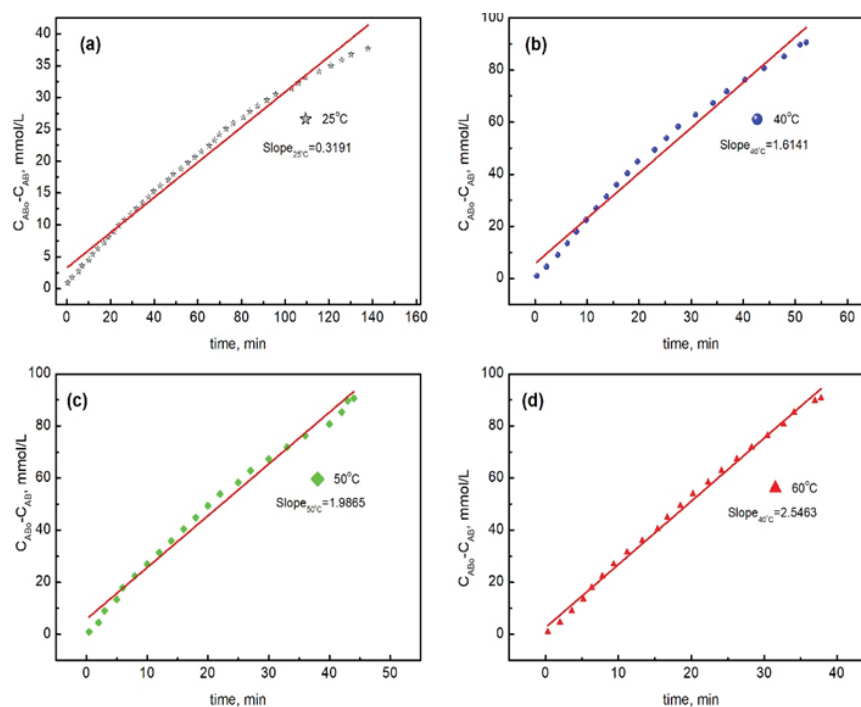
Figure 5. The initial and final ammonia borane concentration differences versus time over NiO@N-rGO at different temperatures.

ons. The as-prepaid NiO@N-rGO exhibits high catalytic performance to the dissociation and hydrolysis of AB at moderate temperature, which is accompanied by a release of up to 3 equivalent H_2 in 40 mins, which could be ascribed to the synergetic effect between NiO NPs and N-rGO. These non-precious metal-free based catalysts with the promoting effect through the nitrogen-doped rGO could open up to find their application not only as promising hydrogen storage materials for onboard systems but also in various other applications.

Acknowledgement

References

[1] Xu, Q., & Chandra, M. (2006). Catalytic activities of non-noble metals for hydrogen generation from aqueous ammonia–borane at room temperature. *Journal of Power Sources, 163*(1), 364-370.

[2] Barış, M., Şimşek, T., Taşkaya, H., & Chattopadhyay, A. K. (2018). Synthesis of Fe-Fe2B catalysts via solvo-thermal route for hydrogen generation by hydrolysis of NaBH4. *Journal of Boron, 3*(1), 51-62.

[3] Çakanyıldırım, Ç., Özsaçmacı, G., & Metin, G. (2016). Co-Mn/TiO2 catalyst to enhance the NaBH4 decomposition. *Journal of Boron, 1*(1), 1-5.

[4] Zhang, H., Zhang, L., Rodríguez-Pérez, I. A., Miao, W., Chen, K., Wang, W., Li, Y., & Han, S. (2021). Carbon nanospheres supported bimetallic Pt-Co as an efficient catalyst for NaBH4 hydrolysis. *Applied Surface Science, 540*(1), 148296.

[5] Balbay, A., Selvitepe, N., & Saka, C. (2021). Fe doped-CoB catalysts with phosphoric acid-activated montmorillonite as support for efficient hydrogen production via NaBH4 hydrolysis. *International Journal of Hydrogen Energy, 46*(1), 425-438.

[6] Abdelhamid, H. N. (2020). Salts induced formation of hierarchical porous ZIF-8 and Their Applications for CO2 Sorption and hydrogen generation via NaBH4 hydrolysis. *Macromolecular Chemistry and Physics, 221*(7), 2000031.

[7] Amri, N. E., & Roger, K. (2020). Polyvinylpyrrolidone (PVP) impurities drastically impact the outcome of nanoparticle syntheses. *Journal of Colloid and Interface Science, 576*, 435-443.

[8] Karaca, T., Sevim, M., & Metin, Ö. (2017). Facile synthesis of monodisperse copper–platinum alloy nanoparticles and their superb catalysis in the hydrolytic dehydrogenation of ammonia borane and hydrazine borane. *ChemCatChem, 9*(22), 4185-4190.

[9] Xu, P., Lu, W., Zhang, J., & Zhang, L. (2020). Efficient hydrolysis of ammonia borane for hydrogen evolution catalyzed by plasmonic Ag@ Pd Core–shell nanocubes. *ACS Sustainable Chemistry & Engineering, 8*(33), 12366-12377.

[10] Shore, S. G., & Parry, R. W. (1955). The crystalline compound ammonia-borane, 1 H3NBH3. *Journal of the American Chemical Society, 77*(22), 6084-6085.

[11] Faverio, C., Boselli, M. F., Medici, F., & Benaglia, M. (2020). Ammonia borane as a reducing agent in organic synthesis. *Organic & Biomolecular Chemistry, 18*, 7789-7813.

[12] Li, H., Yang, Q., Chen, X., & Shore, S. G. (2014). Ammonia borane, past as prolog. *Journal of Organometallic Chemistry, 751*, 60-66.

[13] Vijayalakshmi, K. P., & Suresh, C. H. (2017). Ammonia borane clusters: energetics of dihydrogen bonding, co-operativity, and the Role of Electrostatics. *The Journal of Physical Chemistry A, 121*(13), 2704-2714.

[14] Ren, X., Lv, H., Yang, S., Wang, Y., Li, J., Wei, R., ... Liu, B. (2019). Promoting effect of heterostructured NiO/Ni on Pt nanocatalysts toward catalytic hydrolysis of ammonia borane. *The Journal of Physical Chemistry Letters, 10*(23), 7374-7382.

[15] Zhou, L., Zhang, T., Tao, Z., & Chen, J. (2014). Ni nanoparticles supported on carbon as efficient catalysts for the hydrolysis of ammonia borane. *Nano Research, 7*(5), 774-781.

[16] Zhao, B., Liu, J., Zhou, L., Long, D., Feng, K., Sun, X., & Zhong, J. (2016). Probing the electronic structure of M-graphene oxide (M=Ni, Co, NiCo) catalysts for hydrolytic dehydrogenation of ammonia borane. *Applied Surface Science, 362*, 79-85.

[17] Zhang, J., Chen, C., Yan, W., Duan, F., Zhang, B., Gao, Z., & Qin, Y. (2016). Ni nanoparticles supported on CNTs with excellent activity produced by atomic layer deposition for hydrogen generation from the hydrolysis of ammonia borane. *Catalysis Science&Technology, 6*(7), 2112-2119.

[18] Mahyari, M., & Shaabani, A. (2014). Nickel nanoparticles immobilized on three-dimensional nitrogen-doped graphene as a superb catalyst for the generation of hydrogen from the hydrolysis of ammonia borane. *Journal of Materials Chemistry A, 2*(39), 16652-16659.

[19] Du, X., Liu, C., Du, C., Cai, P., Cheng, G., & Luo, W. (2017). Nitrogen-doped graphene hydrogel-supported NiPt-CeO x nanocomposites and their superior catalysis for hydrogen generation from hydrazine at room temperature. *Nano Research, 10*(8), 2856-2865.

[20] Lu, Y., Huang, Y., Zhang, M., & Chen, Y. (2014). Nitrogen-doped graphene materials for supercapacitor applications. *Journal of Nanoscience and Nanotechnology, 14*(2), 1134-1144.

[21] Hummers Jr., W. S., & Offeman, R. E. (1958). Preparation of graphitic oxide. *Journal of the American Chemical Society, 80*(6), 1339-1339.

[22] Tan, Y.Q., Song, Y.H., & Zheng, Q. (2013). Facile regulation of glutaraldehyde-modified graphene oxide for preparing free-standing papers and nanocomposite films. *Chinese Journal of Polymer Science, 31*(3), 399-406.

[23] Long, D., Li, W., Ling, L., Miyawaki, J., Mochida, I., & Yoon, S.H. (2010). Preparation of nitrogen-doped graphene sheets by a combined chemical and hydrothermal reduction of graphene oxide. *Langmuir, 26*(20), 16096-16102.

[24] Ariharan, A., Viswanathan, B., & Nandhakumar, V. (2017). Nitrogen doped graphene as potential material for hydrogen storage. *Graphene, 6*(2), 41-60.

[25] Yung, T.Y., Huang, L.Y., Chan, T.Y., Wang, K.S., Liu, T.Y., Chen, P.T., ... Liu, L.K. (2014). Synthesis and characterizations of Ni-NiO nanoparticles on PDDA-modified graphene for oxygen reduction reaction. *Nanoscale Research Letters, 9*(1), 444.

[26] Klug, H. P., & Alexander, L. E. (1974). *X-ray diffraction procedures: for polycrystalline and amorphous materials*. (2nd Edition). John Wiley&Sons. ISBN: 978-0-471-49369-3.

[27] Naveen, A. N., & Selladurai, S. (2015). Novel low temperature synthesis and electrochemical characterization of mesoporous nickel cobaltite-reduced graphene oxide (RGO) composite for supercapacitor application. *Electrochimica Acta, 173*, 290-301.

[28] Tao, H.C., Yang, X.L., Zhang, L.L., & Ni, S.-B. (2015). One-step synthesis of nickel sulfide/N-doped graphene composite as anode materials for lithium ion batteries. *Journal of Electroanalytical Chemistry, 739*, 36-42.

[29] Li, G., & Zhang, Y. (2019). Highly selective two-electron oxygen reduction to generate hydrogen peroxide using graphite felt modified with N-doped graphene in an electro-Fenton system. *New Journal of Chemistry, 43*(32), 12657-12667.

[30] Salavati-Niasari, M., & Entesari, M. (2012). Controlled synthesis of spherical α-Ni(OH)2 hierarchical nanostructures via a simple hydrothermal process and their conversion to NiO. *Polyhedron, 33*(1), 302-309.

[31] Chen, X. A., Chen, X., Zhang, F., Yang, Z., & Huang, S. (2013). One-pot hydrothermal synthesis of reduced graphene oxide/carbon nanotube/α-Ni(OH)2 composites for high performance electrochemical supercapacitor. *Journal of Power Sources, 243*, 555-561.

[32] Deng, D., Pan, X., Yu, L., Cui, Y., Jiang, Y., Qi, J., ... Xue, Q. (2011). Toward N-doped graphene via solvothermal synthesis. *Chemistry of Materials, 23*(5), 1188-1193.

[33] Liu, L., Chen, R., Liu, W., Wu, J., & Gao, D. (2016). Catalytic reduction of 4-nitrophenol over Ni-Pd nanodimers supported on nitrogen-doped reduced graphene oxide. *Journal of Hazardous Materials, 320*, 96-104.

[34] Su, F., Lv, X., & Miao, M. (2015). High-performance two-ply yarn supercapacitors based on carbon nanotube yarns dotted with Co3O4 and NiO nanoparticles. *Small, 11*(7), 854-861.

[35] McIntyre, N., & Cook, M. (1975). X-ray photoelectron studies on some oxides and hydroxides of cobalt, nickel, and copper. *Analytical Chemistry, 47*(13), 2208-2213.

[36] Zhou, Q., Yang, H., & Xu, C. (2016). Nanoporous Ru as highly efficient catalyst for hydrolysis of ammonia borane. *International Journal of Hydrogen Energy, 41*(30), 12714-12721.

[37] Xi, P., Chen, F., Xie, G., Ma, C., Liu, H., Shao, C., ... Zeng, Z. (2012). Surfactant free RGO/Pd nanocomposites as highly active heterogeneous catalysts for the hydrolytic dehydrogenation of ammonia borane for chemical hydrogen storage. *Nanoscale, 4*(18), 5597-5601.

[38] Amali, A. J., Aranishi, K., Uchida, T., & Xu, Q. (2013). PdPt nanocubes: a high-performance catalyst for hydrolytic dehydrogenation of ammonia borane. *Particle*

& Particle Systems Characterization, 30(10), 888-892.

[39] Cao, C. Y., Chen, C. Q., Li, W., Song, W. G., & Cai, W. (2010). Nanoporous nickel spheres as highly active catalyst for hydrogen generation from ammonia borane. *ChemSusChem, 3*(11), 1241-1244.

[40] Metin, Ö., Mazumder, V., Özkar, S., & Sun, S. (2010). Monodisperse nickel nanoparticles and their catalysis in hydrolytic dehydrogenation of ammonia borane. *Journal of the American Chemical Society, 132*(5), 1468-1469.

[41] Kalidindi, S. B., Indirani, M., & Jagirdar, B. R. (2008). First row transition metal ion-assisted ammonia−borane hydrolysis for hydrogen generation. *Inorganic Chemistry, 47*(16), 7424-7429.

[42] Umegaki, T., Yan, J.M., Zhang, X.B., Shioyama, H., Kuriyama, N., & Xu, Q. (2009). Preparation and catalysis of poly(N-vinyl-2-pyrrolidone) (PVP) stabilized nickel catalyst for hydrolytic dehydrogenation of ammonia borane. *International Journal of Hydrogen Energy, 34*(9), 3816-3822.

[43] Du, X., Yang, C., Zeng, X., Wu, T., Zhou, Y., Cai, P. ... Luo, W. (2017). Amorphous NiP supported on rGO for superior hydrogen generation from hydrolysis of ammonia borane. *International Journal of Hydrogen Energy, 42*(20), 14181-14187.

[44] Manna, J., Akbayrak, S., & Özkar, S. (2017). Nickel(0) nanoparticles supported on bare or coated cobalt ferrite as highly active, magnetically isolable and reusable catalyst for hydrolytic dehydrogenation of ammonia borane. *Journal of Colloid and Interface Science, 508*, 359-368.

[45] Yang, X. J., Li, L. L., Sang, W. L., Zhao, J. L., Wang, X. X., Yu, C. ... Tang, C. C. (2017). Boron nitride supported Ni nanoparticles as catalysts for hydrogen generation from hydrolysis of ammonia borane. *Journal of Alloys and Compounds, 693*, 642-649.

[46] Lin, Y., Yang, L., Jiang, H., Zhang, Y., Cao, D., Wu, C. ... Song, L. (2019). Boosted reactivity of ammonia borane dehydrogenation over Ni/Ni2P heterostructure. *The Journal of Physical Chemistry Letters, 10*(5), 1048-1054.

[47] Liu, Y., Zhang, J., Liu, Q., & Li, X. (2020). TiN nanotube supported Ni catalyst Ni@ TiN-NTs: experimental evidence of structure–activity relations in catalytically hydrolyzing ammonia borane for hydrogen evolution. *RSC Advances, 10*(61), 37209-37217.

[48] Ghosh, S., Kadam, S. R., Houben, L., Bar-Ziv, R., & Bar-Sadan, M. (2020). Nickel phosphide catalysts for hydrogen generation through water reduction, ammonia-borane and borohydride hydrolysis. *Applied Materials Today, 20*, 100693.

[49] Feng, K., Zhong, J., Zhao, B., Zhang, H., Xu, L., Sun, X., & Lee, S. T. (2016). CuxCo1−xO Nanoparticles on graphene oxide as a synergistic catalyst for high-efficiency hydrolysis of ammonia–borane. *Angewandte Chemie, 128*(39), 12129-12133.